Simulation of electron behavior in PIG ion source for 9 MeV cyclotron

X. J. Mu[1] M. Ghergherehchi[1] Y. H. Yeon[2] J. W. Kim[1] J. S. Chai[1;1)]

[1] College of Information & communication Engineering, School of Electronic and Electrical Engineering, Sungkyunkwan University, Suwon, Korea
[2] Department of Energy Science, Sungkyunkwan University, Suwon, Korea

Abstract: In this paper, we focus on a PIG source for producing intense H-ions inside a 9 MeV cyclotron. The properties of the PIG ion source were simulated for a variety of electric field distributions and magnetic field strengths using a CST particle studio. After analyzing the secondary electron emission (SEE) as a function of both magnetic and electric field strengths, we found that for the modeled PIG geometry, a magnetic field strength of 0.2 T provided the best results in terms of the number of secondary electrons. Furthermore, at 0.2 T, the number of secondary electrons proved to be greatest regardless of the cathode potential. Also, the modified PIG ion source with quartz insulation tubes was tested in a KIRAMS-13 cyclotron by varying the gas flow rate and arc current, respectively. The capacity of the designed ion source was also demonstrated by producing plasma inside the constructed 9 MeV cyclotron. As a result, the ion source is verified as being capable of producing an intense H^- beam and high ion beam current for the desired 9 MeV cyclotron. The simulation results provide experimental constraints for optimizing the strength of the plasma and final ion beam current at a target inside a cyclotron.

Key words: PIG ion source, CST particle studio, electromagnetic field，secondary electron gas flow rate, arc current

PACS: 29.20.dg, 29.25.Ni **DOI:** 10.1088/1674-1137/38/12/127004

1 Introduction

Ion sources are used for producing intense ion beams in various accelerators. The PIG ion source is well known as an internal ion source inside a cyclotron. It derives its name from the vacuum gauge invented by Penning [1].

Computer simulation of a charged particle beam is an important tool for scrutinizing the processes occurring in various fields of physics [2, 3]. Multiple computer simulations by different codes in ion source have been done before, and the simulation results are useful for identification and improvement of ion source devices. Simulation of H^- ion source extraction systems is performed using ion beam simulator IBSIMU developed at the University of Jyvaskyla. The simulation results and experimental data were in good agreement [4, 5]. Other researchers have also demonstrated good experimental and simulation agreement when considering an improved PIG ion source with hydrogen particles within the KIRAMS-13 cyclotron. Thus, the simulation results repeatedly confirm that optimizing the ion source structure and applied field strengths plays a critical role in the good operation of the cyclotron [6].

Therefore, in this paper, we used the CST PARTICLE STUDIO (CST PS) [7] to do the simulation and analysis of electron behavior in a PIG ion source for a 9 MeV cyclotron. The objective of the PIG ion source simulation within CST PS is to obtain constrains on the electric potential at the cathode and the magnetic field to gain high density plasma. We note that while visualizing the electron trajectories and determining SEE characteristics is one part of the ion source operation, a comprehensive analysis requires the inclusion of the electron interaction effect with the target gas, which was not done here. Igniting and sustaining dense plasma requires that enough high energy electrons are present in the system to replenish those lost from interacting with the neutral gas. As part of the simulations, we varied the magnetic field and electric field to try to optimize the production of secondary electrons, finding an optimum magnetic field strength of 0.2 T. The KIRAMS-13 cyclotron, which produces a 13 MeV energy ion beam, was developed by the Korea Institute of Radiological Medical Sciences (KIRAMS) [8] to produce short-lived positron emission tomography radioisotopes for medical diagnosis and treatment. It is used at more than five regional cyclotron centers in South Korea. The maximum produced beam current is limited to the expected value, due to

Received 27 December 2013

1) E-mail: jschai@skku.edu

low efficiency in ion source performance. Multiple investigations to evaluate the ion beam current were studied and performed in previous work [6, 8–11].

2 Technical parameters between 13 MeV and 9 MeV cyclotrons

The main parameters of the 13 MeV cyclotron and 9 MeV cyclotron are illustrated and compared in Table 1. While the shape of the magnet inside a cyclotron is an essential consideration that could affect beam acceleration, however the PIG ion source here is unaffected by these changes.

To compare any possible effect on the PIG ion source designed in this study, here we compare the essential parameters that determine the ion source ionization process for the 9 MeV and 13 MeV cyclotron systems. Both of the vacuum pressures inside these two cyclotrons are provided by diffusion pumps, which are capable of making 10^{-7} Torr pressure in 1 h. The magnetic field distributed at the central region provides a homogenous magnetic field for the ionization process inside the PIG ion source, which is approximately the same value (1.99 T, 1.89 T). The Dee voltage connected to the central region provides the extraction voltage on the puller to extract a H^- beam from the ion source, which is 40 kV and 45 kV. Therefore, by demonstrating the ion beam extraction capabilities from the aperture on the anode in the 13 MeV system, we have shown that the source can successfully work in other systems with different acceleration voltages, such as the desired 9 MeV cyclotron.

Table 1. Main parameters of the 13 MeV and 9 MeV PET cyclotrons.

parameter	13 MeV cyclotron	9 MeV cyclotron
maximum energy/MeV	13	9
beam species	negative hydrogen	negative hydrogen
ion source	PIG/Internal	PIG/Internal
maximum B field/T	1.99	1.89
central B field/T	1.288	1.36
vacuum pumps	diffusion pumps	diffusion pumps
radio-frequency/MHz	71.5	83
dee voltage/kV	40	45
harmonic number	4	4
ion extraction	stripper foil	stripper foil
cooling system	water cooling	water cooling

3 Simulation procedure in CST PS

CST PS is a software tool for three-dimensional design and investigation of charged particle trajectories in the presence of an electromagnetic field [8]. In the PIG ion source operation, the emission of secondary electrons is an important parameter determining the behavior and efficiency of plasma generation. There are three basic types of secondary electrons: backscattered, re-diffused secondary and elastic reflected electrons [12]. We note that CST PS utilizes a model by Furman and Pivi [13], and is a well-known simulation environment for analyzing the generation of secondary electrons.

The model of the PIG ion source was drawn based on the geometry of a typical PIG ion source. The geometry of the model and intensity of the electric and magnetic fields were defined firstly, along with other necessary components including cathode, anode, cathode holder, pocket and cover. The cathodes were 7 mm in diameter and 2.0 mm in thickness, and were screwed into the cathode holders. The cylinder-shaped anode with 20 mm in length having different internal diameters of 6.16 mm to 10.1 mm, was used in the simulation.

The anode was selected as SEE copper and the cathodes were chosen as tantalum material. Note that due to material parameter definition, the secondary electron emission only occurs on the inside surface of the anode, although in a real experimental setting emission, it will also occur at the cathode/anticathodes. The pocket, cathode holds and cover parts were set as aluminum, which is non-magnetic. Further, all conducting materials were defined as perfect electrically conducting (PEC), while using a vacuum as the background material corresponding to an experimental environment.

As all the components for the electrostatic part were defined, we opted to simulate the electric potential from 100 V up to 2500 V, while considering the magnetic field strengths of 0.2, 0.4, and 0.6 T. These values were chosen due to experimental lab constraints, and also due to previous work for a separate (but similar) geometry in the literature [14]. To apply a magnetic field in a PIG, either a permanent magnet or an electromagnetic coil can be utilized experimentally. For CST, an electromagnetic coil implantation was utilized, with magnetic fields defined by the number of coil turns N and electric current I, based on Eq. (1).

$$NI=\oint\frac{B}{\mu}\mathrm{d}l=B\times\frac{l_1}{\mu_0}+B\times\frac{l_2}{\mu}\approx B\times\frac{l_1}{\mu_0}, \qquad (1)$$

where: l_1=the length of gap between two cathodes, μ_0= the permeability in air, and B=magnetic field intensity. (B=0.2 T in the experimental permanent magnet).

The initial seed electrons were set up after definition of the electric and magnetic fields. The seed electrons were then set to fixed emission from the cathode surfaces as shown in Fig. 1 (purple dots). Particle trajectories were calculated within the particle track simulation workflow with a time-step defined by the fastest particle in the simulation (i.e. the time steps will not be constant).

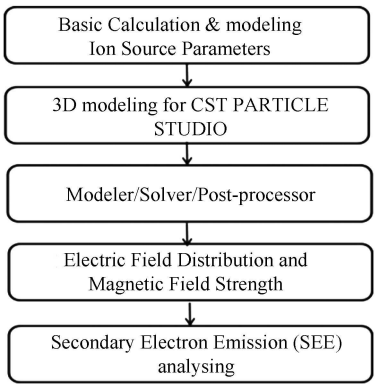

The simulation setup model.

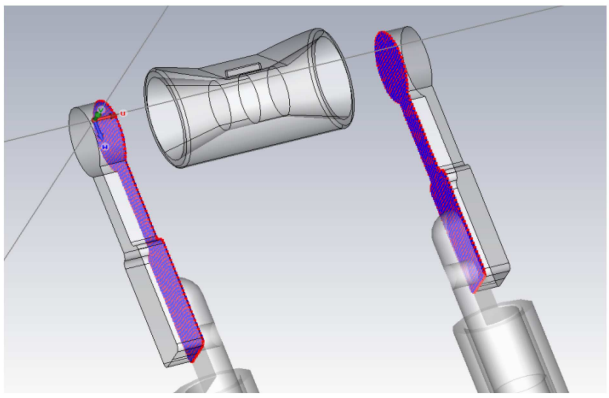

Fig. 1. Particle source from cathode surfaces.

4 Results and discussion

4.1 Electron trajectory

Firstly, we demonstrate visualization of the electron trajectories in a −1000 V electric field and 0.1 T density magnetic field for the PIG ion source in Figs. 2(a) and 2(b) respectively. The magnetic field is homogeneously distributed, and the two fields are almost parallel to each other.

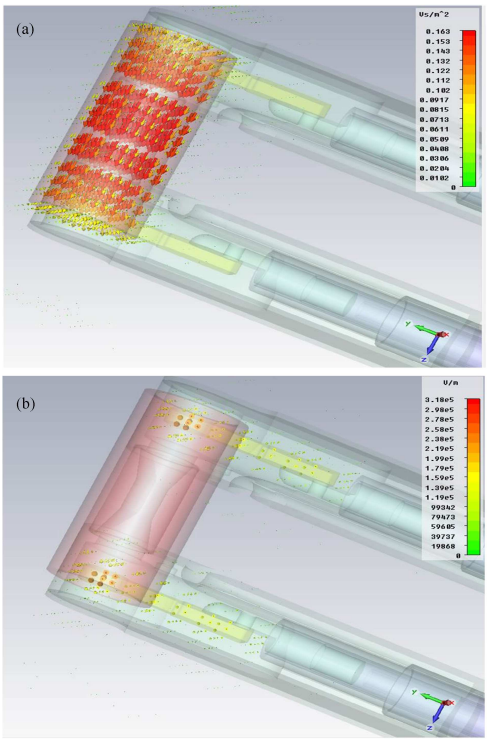

Fig. 2. The electron trajectories plotted in (a) 0.1 T magnetic field and (b) −1000 V electric field.

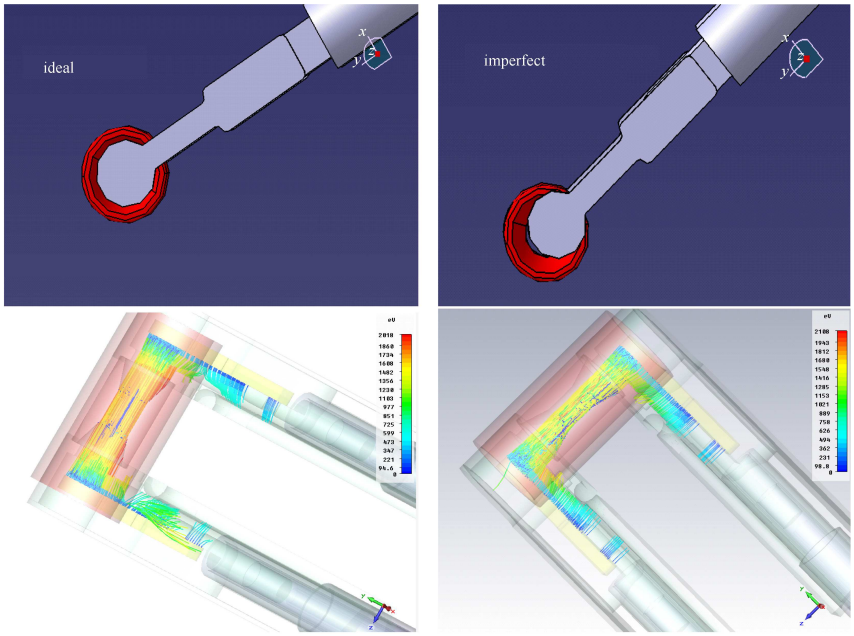

Fig. 3. Geometry and electron trajectories corresponding to ideal and imperfect geometry.

Prior to considering the effect of magnetic field and electric field on the formation of secondary electrons, we examined the effect of an off-center cathode positioning with respect to the anode and magnetic coil. As could be expected, the properly aligned configuration produces significantly more secondary emission electrons because the diameter of electron trajectory is bigger, as seen in Fig. 3. It was also observed that the lifetime of the secondary electrons was also longer, due to better confinement of the electrons.

Next the effect of varying the electrical field, while holding the magnetic field strength constant, was considered. High density electrons, which can make many electron-neutral collisions happen, are required for efficient ionization of a neutral gas. Further, electron energy should be several times the magnitude of the neutral atom ionization potential. Since directly this condition is difficult to achieve, an abundance of secondary electrons must be emitted to reach a higher energy than the primary electrons. To illustrate the dependence of SEE on the cathode potential, Fig. 4 shows the number of secondary electrons (each simulation has the same density/number of particle sources from the cathode, thus the number of secondary electrons is comparable) for voltages −100 V to −2500 V at the cathode, and for B=0.2, 0.4, and 0.6 T. The graph clearly shows that at B=0.2 T, the greatest number of secondary electrons are produced. However, as a function of the electric potential, the 0.4 T magnetic field produces a more consistent/stable number of secondary electrons. As the magnetic field is further increased, the SEE counts drop considerably, as can be seen for 0.6 T. We also plot the secondary electron kinetic energy as a function of the applied cathode potential at 0.2 T in Fig. 5. It is observed that the kinetic energy is increased as the value of electric field increases.

Therefore, for the geometry considered in this paper, a suggested magnetic field strength for SEE is 0.2 T. This result and the simulation data, while not suggestive of an optimal plasma-generation condition, can be utilized for future simulations including the effect of neutral gas ionization effects.

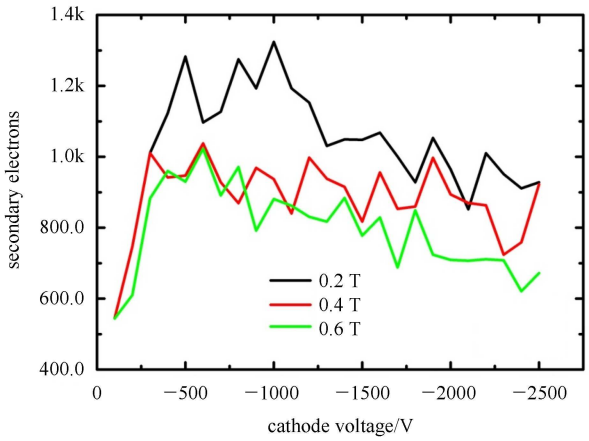

Fig. 4. Voltage applied to cathode vs number of secondary electron in 0.2 T, 0.4 T, 0.6 T magnetic field.

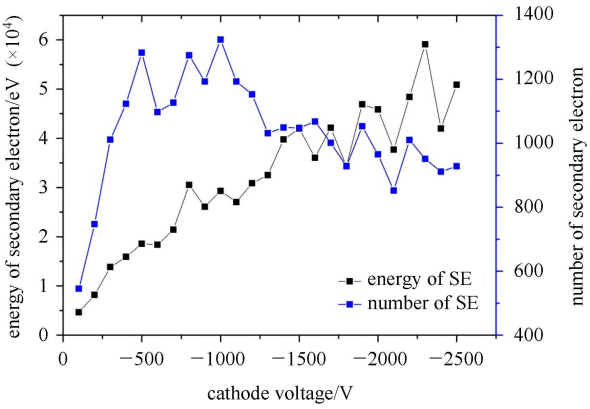

Fig. 5. Energy of secondary electrons in 0.2 T magnetic field.

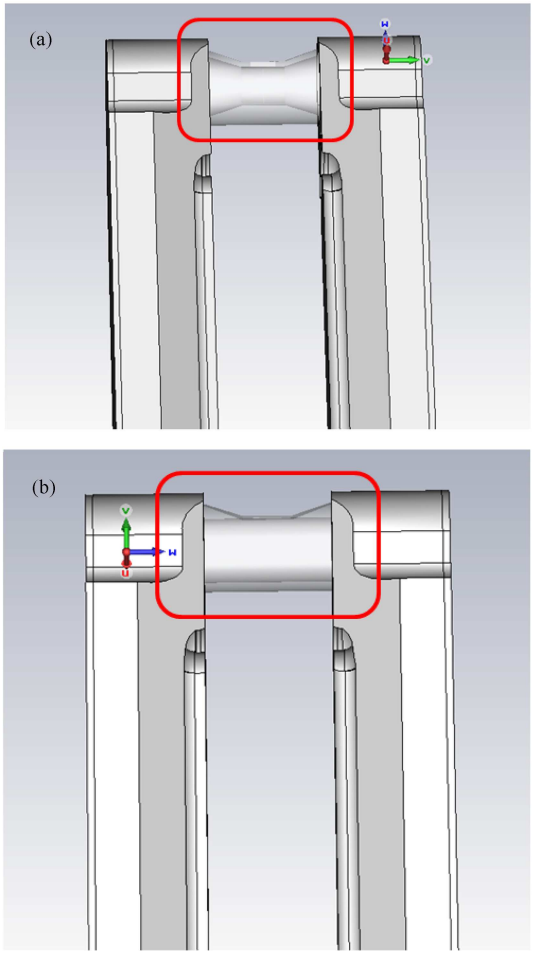

Fig. 6. PIG ion source with (a) Designed anode and (b) inner cylinder shape anode.

4.2 Anode geometry in CST PS

The anode was designed as illustrated in Fig. 6. To verify its advantage, this designed anode and the prototype in cylinder shape were modeled in this work using CST PS. The number of secondary electrons in these two anodes varied by the different density of electric fields is demonstrated in Fig. 7, where three times more secondary electrons are produced by using the new designed anode compared with the cylinder one. Consequently, the designed anode, which can produce a bigger amount of higher energy secondary electrons, is proved to produce a higher density of plasma since it makes higher ionization probability.

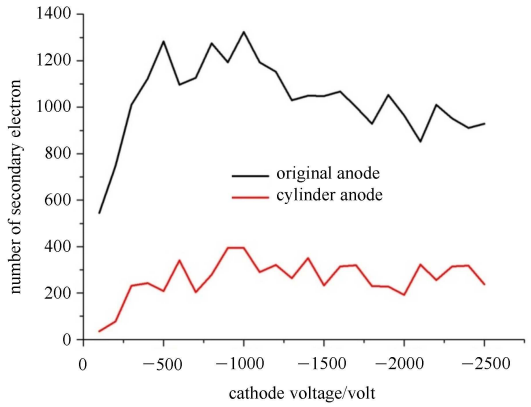

Fig. 7. Number of secondary electrons vs. cathode voltages in two types of anodes.

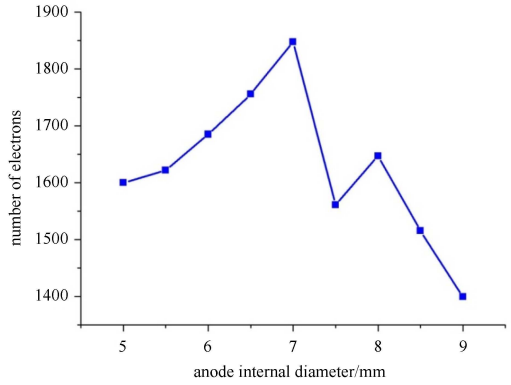

Fig. 8. Simulation results of anode with various inner diameters.

Herein the evaluation of secondary electron emission by varying the inner diameter of the anode is also simulated using CST PS. The prototype anode is 6.16 mm in inner diameter. The electron distribution is calculated as a function of anode inner diameter while being placed in a 2000 V electric field and 1.36 T magnetic field, as illustrated by Fig. 8 for a fixed value of emitted electrons. As a result in this work, the anode with 7 mm in inner diameter is demonstrated to be capable of producing the highest density of electrons while the 8 mm inner diameter anode gives the highest beam current density in KIRAMS-13. Fig. 8 also shows that when the anode with an inner diameter higher than 9 mm is used, the number of electrons produced will decrease, this means the reduction of secondary electron production efficiency.

4.3 Ion beam extraction in CST PS

In order to optimize the beam emission from the central region to the acceleration region, ion beam extraction from the ion source side wall aperture through a typical puller was modeled using CST PS. The H^- beam was extracted under the following experimental constraints based on the KIRAMS-13 cyclotron: −2.5 kV voltage on cathodes by the arc power supply, 45 kV voltage on pullers from Dee voltage, and a 1.288 T center homogeneous magnetic field [6]. As a simulation result, the relative location of pullers to ion source is fixed at the distance of 2.2 mm between the center of two pullers and the anode aperture in the horizontal direction. By rotating the anode, it is found that the ratio of beam extraction through the puller is a distribution over the anode rotation angles. The ion beam extracted from the slit on the anode wall through puller enters the acceleration region inside the cyclotron, and part of the beam is lost because of the beam diffusion flow in the central region (Fig. 9). It is demonstrated from Fig. 10 that with the anode rotation angles from −0.2° to −1.5°, more than 50% H^- beam can be extracted through pullers. The H^- beam extraction trajectory is shown in Fig. 9. The simulation result is useful for optimizing the future beam extraction from the puller in the 9 MeV cyclotron.

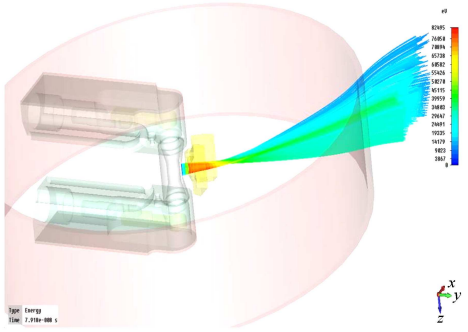

Fig. 9. Extracted ion trajectory through pullers.

4.4 Test and measurement of modified PIG ion source in KIRAMS-13 cyclotron

The ion source with new designed insulator tubes was tested and measured in a KIRAMS-13 cyclotron. The relative angle between the ion source and puller was fixed at 30° while the relative angle between the slit and puller was fixed at 1.5° based on the CST simulation results. Beam currents at the carbon foil and the target

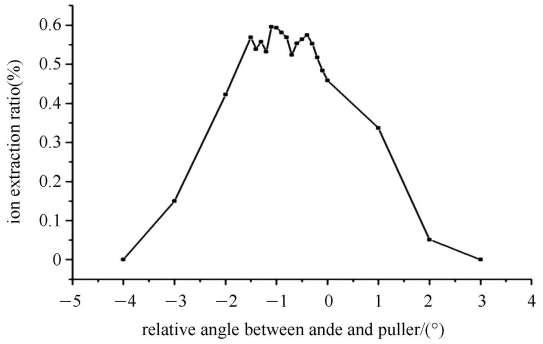

Fig. 10. Ion extraction ratio vs. anode rotation angles.

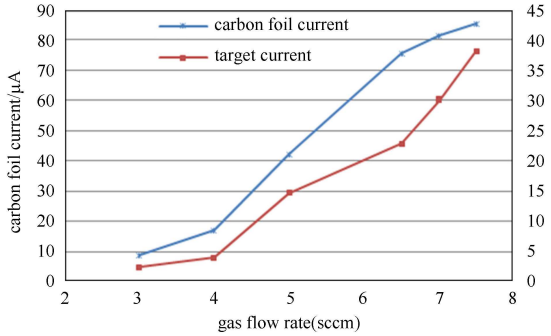

Fig. 11. Beam current at carbon foil and target vs. gas flow rate.

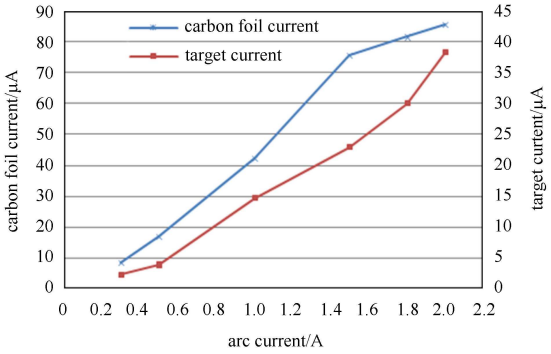

Fig. 12. Beam current at carbon foil and target vs. arc current.

according to the gas flow rate and arc current were measured. The results are shown in Figs. 11, 12, respectively. It is verified that the beam current at the carbon foil or target is increased when both the gas flow rate and the arc current are increased. To investigate the influence of the two factors in the ion source performance, one factor was fixed while the other one was varied. As illustrated in Fig. 12, the arc current induces a weaker effect (by percentage change) on the beam current at both the carbon foil and the target when compared with simply varying the gas flow rate. The maximum beam current measured at the target was 48.3 micro amperes under 2.0 ampere arc current and 7.5 sccm hydrogen gas flow rate.

5 Conclusion

We optimized the experimental facilities using both simulations and experiments. A computer simulation of the electron trajectory in the PIG ion source for 9 MeV cyclotron was successfully implemented in the CST PARTICLE STUDIO. The dependence of SEE on cathode potential and confining magnetic field strength were also examined, with the greatest SEE occurring for 0.2 T. The result is helpful for future simulation and experiment to generate a high density of plasma and high ion beam current. The behavior of electrons, modification of ion source geometry and optimization of H^- beam extraction were modeled in the CST PARTICLE STUDIO. The simulation results provide experimental constraints for optimizing the plasma strength and beam current inside a cyclotron. The modified ion source was tested at different gas flow rates and arc currents in the KIRAMS-13 cyclotron, and it was demonstrated that gas flow rate and arc current play important roles in the H^- beam current. Moreover, the ion beam extraction capabilities from the aperture on the anode wall were demonstrated. We note a PIG ion source in a 9 MeV cyclotron at Sungkyunkwan University constructed from the same design was recently shown to successfully produce a beam.

This work was supported by the Korea Evaluation Institute of Industrial Technology (KEIT) funded by the Ministry of Trade, Industry & Energy (10043897, Development of 500 cGy level radiation therapy system based on automatic detection and tracing technology with dual-head gantry for 30% reducing treatment for cancer tumors).

References

1 Penning F M. Physica., 1973, **4**: 71
2 Litovko I, Oks E. Proc. of the 33th EPS Conf. on Plasma Physics, Rome: 301. 2006. 104
3 Mitsi Tet al. Appl. Surf. Sci., 2001, **747**: 169
4 Kalvas T et al. Rev. Sci. Instrum., 2012, **83**: 02A705
5 Kalvas T et al. Rev. Sci. Instrum., 2010, **81**: 02B703
6 Lee B C et al. J. Korean Phys. Soc., 2010, **57**: 1376
7 CST. http://www.cst.com/
8 An D H et al.Rev. Sci. Instrum., 2008, **79**: 02A520
9 An D H, Chai J S.17th International Conf. on Cyclotrons and Their Applications. Tokyo, Japan. 2004
10 Kim Y S et al. Proc. of the 3rd Particle Accelerator. APAC2004, Korea: 2004. TUP13008
11 An D H et al. Proc. of the 3rd Particle Accelerator. APAC2004, Korea: 2004. MOP15014
12 Hamme F et al. Proc. of ICAP 2006. France: 2006. TUAPMP04
13 Furman M A, Pivi M T F. Phys. Rev. ST Accel. Beams., 2002, **5**: 124404
14 Jimbo K et al. Nucl. Instrum. Methods A, 1986, **248**: 282